

# Voltage Stability Assessment from Massive Steaming PMU Data using Multiple High-Dimensional Covariance Test

Lei Chu<sup>2</sup>, Robert Qiu<sup>1,2</sup>, Xing He<sup>2</sup>, Zenan Ling<sup>2</sup>, Yadong Liu<sup>2</sup>

<sup>1</sup> Department of Electrical and Computer Engineering, Tennessee Technological University, Cookeville, TN 38505 USA.

<sup>2</sup> Department of Electrical Engineering, Research Center for Big Data Engineering Technology, State Energy Smart Grid Research and Development Center, Shanghai Jiaotong University, Shanghai 200240, China.

**Abstract**—Analogous deployment of phase measurement units (PMUs), deregulation of energy market and the urge for power system state estimation, all call for voltage stability assessment in modern power system. Implementing a model based estimator though is impracticable as the complexity scale of solving the high dimension power flow equations. In this paper, we firstly represent massive streaming PMU data as big random matrix flow. Motivated by exploiting the variations in the covariance matrix of the massive streaming PMU data, a novel voltage stability assessment algorithm is then developed based on the multiple high dimensional covariance test. The proposed test statistic is nonparametric without assuming a specific parameter distribution for the PMU data and of a wide range of data dimensions and sample size. Besides, it can jointly reveal the relative magnitude, duration and location of an system event. For the sake of practical application, we reduce the computation of the proposed test statistic from  $O(\varepsilon n_g^4)$  to  $O(\eta n_g^2)$  by principal component calculation and redundant computation elimination. The novel algorithm is numerically evaluated utilizing the IEEE 30-, 118-bus system and a Polish 2383-bus system and a real 34-PMU system. The case studies illustrate and verify the superiority of proposed voltage stability indicator.

**Index Terms**—Power System, Voltage Stability Assessment, Massive Streaming PMU Data, Multiple High-dimension Covariance Test.

## I. INTRODUCTION

**R**ELIABLE operation and intelligent management of electric power systems influences heavily on everyday life. Recently, power companies, scholars and researchers keep their eyes on utilizing PMUs to improve wide area monitoring, protection and control (WAMPAC) [1, 2]. Some large-scale implementations of synchrophasor technology in managing the power grid across the world have been brought online. For an illustration, there were about 2400 PMUs deployed in power grids in China as of 2013 [3]; North America and India have coverage from about 2000 and 1800 PMUs by 2015, respectively [4]. Accordingly, designing, monitoring and controlling such systems are becoming increasingly more challenging as a consequence of the steady growth of their size, complexity, level of uncertainty, unpredictable behavior, and interactions [5, 6].

Efforts are in place to take synchrophasor technology into assess voltage stability and develop reliable operational pro-

cedures to better understand and manage the power grid with wide-area visualization tools using PMU data. These voltage stability assessment methods can be generally organized into two categories: model-based estimators and data driven estimators. Model-based analysis is a kind of traditional method for offline analysis of voltage stability in power systems. Lof and Anderson presented statistic voltage stability indices based on the largest singular value of the inverse of the power flow Jacobian matrix [7]. Ghiocel and Chow extend the result in [7] and identify power flow control infeasibilities in a large-scale power system [8]. Pordanjani, Wang and Xu assess the voltage stability using Channel components transform [9]. More recently, equivalent nodal analysis for voltage stability assessment is shown in [10]. With the help of eigenvalues, eigenvectors, and participation factors of the power flow Jacobian matrix, the system characteristics can be predicted by these estimators. However, they hardly meets the severe requirements for efficient and stable monitoring of dynamically changed power systems possessing the steady growth of their size, complexity and unpredictable behaviors.

As a novel alternative on the other hand, the lately advanced data driven estimator can assess voltage stability without knowledge of the power network parameters or topology [11–16]. Xie, Chen and Kumar proposed a linearized analysis algorithm for early event detection using the reduced dimensionality [12]. Lim and DeMarco presented a SVD-based voltage stability assessment from PMU data, but their methods would be hardly implemented for real time assessment in a large power system due to the high computation burden [13]. Instead of monitoring the raw PMU data, the statistics of the PMU measurements arouse considerable interest recently. Ghanavati, Hines and Lakoba sought to identify a statistical voltage stability indicator by calculating the expected variance and autocorrelation of the buses voltages and currents [14]. It is noted that the success of these approaches requires an accurate statistical model of measurement noise and load fluctuations. Besides, the constraint that the data dimension should be smaller than the window size is also to be satisfied in [12, 13]. On the other hand, linear eigenvalue statistics (LESS) of the high-dimensional PMU data were utilized for situation awareness or correction analysis of power system in our recent

works [11, 15, 16]. Taking advantage of asymptotic properties of high-dimensional random matrix, LES-based methods provided robust voltage stability assessment using individual window-truncated PMU data. Rather than exploiting individual window-truncated PMU data, this work seeks to indicate voltage stability by high-dimensional statistical properties of overall PMU data.

Besides, from the perspective of theoretical research, large deployment of synchronized PMU raises several open issues:

- 1) How to represent the massive streaming PMU data in the manner of continuous learning of power system?
- 2) How to evaluate the real time voltage stability from massive streaming PMU data?
- 3) Is there any method that can turn the big PMU data into tiny data for the practical use?
- 4) How to develop a voltage stability estimator without assuming a specific parametric distribution for the data?
- 5) Is there exist a flexible data driven voltage stability indicator with a wide range of dimensions and sample size?

A new metric proposed here is based on multiple high dimensional covariance test. Test about the high-dimensional covariance matrix has increasingly its popularity recently. The first attempt on the high-dimensional covariance matrix test presented by Bai and Saranadasa was based on likelihood ratio (LR) test [17]. The LR test worked well for normally distributed data on condition that the sample size was larger than the data dimension. Gupta and Xu extended the LR test to non-normal distribution [18] while Bai et al. [19] considered a correction of the LR (CLR) test in case of a wide range of data dimension. These tests shared basic assumption that the population covariance matrix can be directly substituted by the sample covariance matrix. However, genomic studies shown that such a assumption may not work as these sample covariance matrix based estimators had unnecessary terms which slowed down the convergence considerably as the dimension is high [20–22]. Instead of estimating the population covariance matrix directly, some well-defined distance were proposed to evaluate the difference among populations [22]. Ledoit and Wolf exploited scaled trace-based distance measure between two sub-populations when the data dimension is large compared to the sample size [20]. By exploiting the merits of U-statistics [23], Chen etc. extended the results in [20] with a wide range of data dimension and sample size. However, these works were of high computation burden and focused on the difference of two sub-populations which made them unsuitable for indicating real time voltage stability in case of massive streaming PMU data.

In this paper, by exploiting the changes in the covariance matrix of different sampling period of the streaming PMU data, we develop a novel voltage stability assessment algorithm using the multiple high dimensional covariance test. The key features of the proposed test statistic are: 1) it can jointly reveal the relative magnitude, duration (or so-called clearing time) and location of an system event; 2) it specifies no parameter distribution of the PMU data which implies a wide range of the practical applications; 3) it is a real time data driven method

without requiring any knowledge of the the system model or topology; 4) it is a flexible voltage stability indicator without specifying an explicit relationship between data dimension and sample size. 5) it provides effective computation due to principal component calculation and redundant computation elimination. 6) it implements the asymptotic properties of the high dimensional PMU data to enhance the robustness of the test statistic;

The remainder of this paper is structured as follows. Section II introduces the representation of massive streaming PMU data. Section III presents a voltage assessment approach using multiple high dimension covariance test. By principal component calculation and redundant computation elimination, an effective calculating method for the proposed test statistic is also developed. In Section IV, numerical case studies using synthetic data and real data are provided to evaluate the performance of the proposed voltage stability indicator. Conclusion of this research is given in Section V. For the sake of simplicity, all technical details and some additional case study results are deferred to the Appendices.

## II. MASSIVE STREAMING PMU DATA MODELLING

It is well accepted that the transient behavior of a large electric power system can be illustrated by a set of differential and algebraic equations (DAEs) as follows [24, 25]:

$$\dot{\mathbf{x}}^{(t)} = \mathbf{f}(\mathbf{x}^{(t)}, \mathbf{u}^{(t)}, \mathbf{h}^{(t)}, w) \quad (1)$$

$$0 = \mathbf{g}(\mathbf{x}^{(t)}, \mathbf{u}^{(t)}, \mathbf{h}^{(t)}, w) \quad (2)$$

where  $\mathbf{x}^{(t)} \in \mathbb{C}^{m \times p}$  are the power state variables, e.g., rotor speeds and the dynamic states of loads,  $\mathbf{u}^{(t)}$  represent the system input parameters,  $\mathbf{h}^{(t)}$  define algebraic variables, e.g., bus voltage magnitudes,  $w$  denote the time-invariant system parameters.  $t \in \mathcal{R}$ ,  $m$  and  $p$  are the sample time, number of system variables and bus, respectively. The model-based stability estimators [8, 10, 14, 24, 26] focus on linearization of nonlinear DAEs in (1) and (2) which gives

$$\begin{bmatrix} \Delta \dot{\mathbf{x}} \\ \Delta \dot{\mathbf{u}} \end{bmatrix} = \begin{bmatrix} \mathbf{A} & -\mathbf{f}_{\mathbf{u}} \mathbf{g}_{\mathbf{u}}^{-1} \mathbf{g}_{\mathbf{x}} \\ \mathbf{0} & -\mathbf{E} \end{bmatrix} \begin{bmatrix} \Delta \mathbf{x} \\ \Delta \mathbf{u} \end{bmatrix} + \begin{bmatrix} \mathbf{0} \\ \mathbf{C} \end{bmatrix} \xi, \quad (3)$$

where  $\mathbf{f}_{\mathbf{x}}$ ,  $\mathbf{f}_{\mathbf{u}}$  are the Jacobian matrices of  $\mathbf{f}$  with respect to  $\mathbf{x}$ ,  $\mathbf{u}$  and  $\mathbf{A} = \mathbf{f}_{\mathbf{x}} - \mathbf{f}_{\mathbf{u}} \mathbf{g}_{\mathbf{u}}^{-1} \mathbf{g}_{\mathbf{x}}$ .  $\mathbf{E}$  is a diagonal matrix whose diagonal entries equal  $t_{cor}^{-1}$  and  $t_{cor}$  is the correction time of the load fluctuations.  $\mathbf{C}$  denotes a diagonal matrix whose diagonal entries are nominal values of the corresponding active ( $P$ ) or reactive ( $Q$ ) of loads;  $\xi$  is assumed to be a vector of independent Gaussian random variables.

It is noted that estimating the system stability by solving the equation (3) is becoming increasingly more challenging [2, 5] as a consequence of the steady growth of the parameters, say,  $t$ ,  $p$  and  $m$ . Besides, the assumption that  $\xi$  follows Gaussian distribution would restrict the practical application.

As a novel alternative on the other hand, the lately advanced data driven estimators [11–16] can assess voltage stability without knowledge of the power network parameters or topology. However, these estimators are based on the analysis of individual window-truncated PMU data. In this work, we seek

to provide a method with ability of continuous learning of power system from massive streaming PMU data.

Firstly, we try to turn the big PMU data into tiny data for the practical use. Fig. 1 illustrates the conceptual representation of the structure of the massive streaming PMU data. More specifically, let  $p$  denote the number of the available PMUs across the whole power network, each providing  $c$  measurements. At  $i$ th time sample, a total of  $\kappa = p \times c$  measurements, say  $\mathbf{z}_i$ , are collected. With respect to each PMU, the  $c$  measurements could contain many categories of variables, such as voltage magnitude, power flow and frequency, etc. In this work, we develop PMU data analysis assuming each type of measurements is independent. That is, we assume that at each round of analysis,  $\kappa := p$ . Given  $q$  time periods of  $T$  seconds with  $K$  Hz sampling frequency in  $k$ th data collection. Let  $n_g = T \times K$  and  $\mathbf{Z}_{ig} = \{\mathbf{z}_{i1}, \dots, \mathbf{z}_{in_g}\}$ ,  $i = 1, 2, \dots, n$ , a sequence of large random matrix

$$\left\{ \underbrace{\mathbf{Z}_{11}, \mathbf{Z}_{12}, \dots, \mathbf{Z}_{1q}}_{q \text{ window-truncated data}}, \dots, \underbrace{\mathbf{Z}_{n1}, \mathbf{Z}_{n2}, \dots, \mathbf{Z}_{nq}}_{q \text{ window-truncated data}} \right\} \quad (4)$$

is obtained to represent the collected voltage magnitude data.

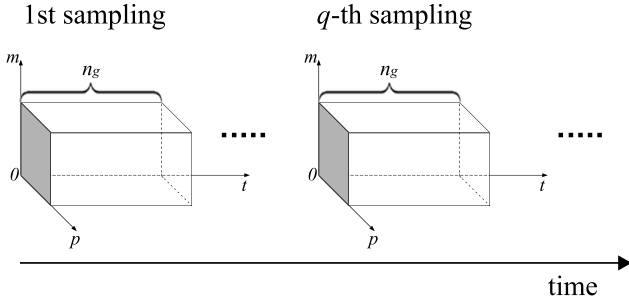


Fig. 1: Conceptual representation of the structure of the massive streaming PMU data.

### III. VOLTAGE STABILITY ASSESSMENT

Once we have validated the random data flow model for the massive streaming PMU data, the next step is to extract the real-time analytics. As we all know, power systems are continually experiencing fluctuations of small magnitudes [25]. In the functional setting, it is of interest to test whether or not  $q$  sets of bus voltage curves have similar variation. For assessing stability when subjected to a specified disturbance, it is reasonable to assume that the system is initially in a steady-state operating condition [25, 27]. Thus it is interesting to discover the difference of the measurements collected in normal condition and abnormal condition by the multiple high dimensional covariance test.

#### A. Multiple High Dimensional Covariance Matrix Test

As depicted in the Section I, a large random matrix flow  $\{\mathbf{Z}_1, \mathbf{Z}_2, \dots, \mathbf{Z}_q\}$  is adopted to represent the massive streaming PMU data in one sample period. Instead of analyzing the raw individual window-truncated PMU data  $\mathbf{Z}_g$  [12, 13] or the

statistic of  $\mathbf{Z}_g$  [11, 14–16], a comprehensive analysis of the statistic of  $\{\mathbf{Z}_1, \mathbf{Z}_2, \dots, \mathbf{Z}_q\}$  is conducted in the following.

More specially, denote  $\Sigma_i$  as the covariance matrix of  $i$ th collected PMU measurements, we want to test the hypothesis:

$$\begin{aligned} H_0 : \Sigma_1 = \Sigma_2 = \dots = \Sigma_q \\ H_1 : \exists j, k \text{ s.t. } \Sigma_j \neq \Sigma_k \end{aligned} \quad (5)$$

#### B. Proposed test statistic

The LR test [17] and CLR test [19] as introduced in the Section I are most commonly test statistics for the hypothesis in (5). For the readers' convenience, we briefly explained the technical details in the Appendix A. These tests can be understood by replacing the population covariance matrix  $\Sigma_g$  by its sample covariance matrix  $\mathbf{Y}_g$ . While direct substitution of  $\Sigma_g$  by  $\mathbf{Y}_g$  brings invariance and good testing properties as shown in [17] for normally distributed data. The test statistic  $V_2$  may not work for high-dimensional data as demonstrated in [20, 21]. Besides, the estimator  $V_3$  has unnecessary terms which slow down the convergence considerably when dimension of PMU data is high [21, 22]. In such situations, to reduce the drawbacks, trace criterion [21] is more suitable to the test problem. Specially, instead of estimating the population covariance matrix directly, a well defined distance measure exploiting the difference among data flow  $\{\mathbf{Z}_1, \mathbf{Z}_2, \dots, \mathbf{Z}_q\}$  is conducted, that is, the trace-based distance measure between  $\Sigma_s$  and  $\Sigma_t$  is

$$\text{tr} \{ (\Sigma_s - \Sigma_t)^2 \} = \text{tr} (\Sigma_s^2) + \text{tr} (\Sigma_t^2) - 2\text{tr} (\Sigma_s \Sigma_t), \quad (6)$$

where  $\text{tr}(\cdot)$  is the trace operator. Instead of estimating  $\text{tr}(\Sigma_s^2)$ ,  $\text{tr}(\Sigma_t^2)$  and  $\text{tr}(\Sigma_s \Sigma_t)$  by sample covariance matrix based estimators, we adopt the merits of the U-statistics [23]. Specially, for  $l = \{s, t\} \in \Omega = \{1 \leq s, t \leq q, s \neq t\}$ ,

$$\begin{aligned} A_l &= \frac{1}{n_g(n_g-1)} \sum_{i \neq j} (\mathbf{z}'_{li} \mathbf{z}_{lj})^2 \\ &- \frac{2}{n_g(n_g-1)(n_g-2)} \sum_{i,j,k}^* \mathbf{z}'_{li} \mathbf{z}_{lj} \mathbf{z}'_{lk} \mathbf{z}_{lk} \\ &+ \frac{1}{n_g(n_g-1)(n_g-2)(n_g-3)} \sum_{i,j,k,h}^* \mathbf{z}'_{li} \mathbf{z}_{lj} \mathbf{z}'_{lk} \mathbf{z}_{lh} \end{aligned} \quad (7)$$

is proposed to estimate  $\text{tr}(\Sigma_l^2)$ . It is noted that  $\sum^*$  represents summation over mutually distinct indices. For example,  $\sum_{i,j,k}^*$  says summation over the set  $\{(i, j, k) : i \neq j, j \neq k, k \neq i\}$ . Similarly, the estimator for  $\text{tr}(\Sigma_s \Sigma_t)$  can be expressed as

$$\begin{aligned} C_{st} &= \frac{1}{n_g^2} \sum_i \sum_j (\mathbf{z}'_{si} \mathbf{z}_{tj})^2 \\ &- \frac{1}{(n_g-1)n_g^2} \sum_{i,h}^* \sum_j \mathbf{z}'_{si} \mathbf{z}_{tj} \mathbf{z}'_{sj} \mathbf{z}_{th} \\ &- \frac{1}{(n_g-1)n_g^2} \sum_{i,l}^* \sum_j \mathbf{z}'_{ti} \mathbf{z}_{sj} \mathbf{z}'_{sj} \mathbf{z}_{th} \\ &+ \frac{1}{(n_g-1)^2 n_g^2} \sum_{i,h}^* \sum_{j,k}^* \mathbf{z}'_{si} \mathbf{z}_{tj} \mathbf{z}'_{sk} \mathbf{z}_{th}. \end{aligned} \quad (8)$$

The test statistic which measures the distance between  $\Sigma_s$  and  $\Sigma_t$  is

$$V_{st} = A_s + A_t - C_{st}. \quad (9)$$

Then the proposed test statistic can be expressed as:

$$V_1 = \frac{1}{q(q-1)} \sum_{\{s,t\} \in \Omega} T_{st}. \quad (10)$$

As  $p, n_g \rightarrow \infty$ , the asymptotic normality [22] of the test statistic (9) is presented in the following:

**theorem III.1.** Let  $\sigma_{st}^2 = \frac{1}{n_g} (A_s + A_t)$ . Assuming the following conditions:

1) For any  $k$  and  $l \in \{s, t\}$ ,  $\text{tr}(\Sigma_k \Sigma_l) \rightarrow \infty$  and

$$\text{tr}\{(\Sigma_i \Sigma_j)(\Sigma_k \Sigma_l)\} = O\{\text{tr}(\Sigma_i \Sigma_j) \text{tr}(\Sigma_k \Sigma_l)\}.$$

2) For  $i = 1, 2, \dots, n_g$ ,  $\mathbf{z}^{(i)}$  are independent and identically distributed  $p$ -dimensional vectors with finite 8th moment.

Under above conditions,

$$L = \frac{V_{st}}{\sigma_{st}} \xrightarrow{d} \mathcal{N}(0, 1)$$

**Proposition III.2.** For any  $q \geq 2$ , as  $p, n_g \rightarrow \infty$ , the proposed test statistic  $V_1$  satisfies

$$V_1 \xrightarrow{d} \mathcal{N}(\mu, \sigma^2), \quad (11)$$

where  $\mu \approx 0, \sigma^2 = \sum^* \sigma_{st}^2$ .

Let  $R = \frac{V_1}{\sigma_{V_1}}$ , the false alarm probability (FAP) for the proposed test statistic can be represented as

$$\begin{aligned} P_{FAP} &= P(R > \alpha | H_0) \\ &= \int_R^\infty \frac{1}{\sqrt{2\pi}} \exp\left(-\frac{t^2}{2}\right) dt \\ &= Q(R), \end{aligned} \quad (12)$$

where  $Q(x) = \int_x^\infty 1/\sqrt{2\pi} \exp(-t^2/2) dt$ . For a desired FAP  $\tau$ , the associated threshold should be chosen such that

$$\alpha = Q^{-1}(\tau).$$

Otherwise, the detection rate (DR) can be denoted as

$$P_{DR} = P(R \geq Q(\alpha) | H_1). \quad (13)$$

It is noted that the computation complexity of proposed test statistic in (11) is  $O(\varepsilon n_g^4)$  which limits its practical application. Here, we proposed a effective approach to reducing complexity of the proposed test statistic from  $O(\varepsilon n_g^4)$  to  $O(\eta n_g^2)$  by principal component calculation and redundant computation elimination. For simplicity, the technical details are deferred to the Appendix B.

### C. Continuous Learning of the Power System

Based on the proposed multiple high-dimensional test (10) in Section III-B, we propose an method in the continuous manner to indicate the voltage stability. Details is shown in the following:

Let

$$T_{trn} = [T_{trn}^{11}, \dots, T_{trn}^{1q}, \dots, T_{trn}^{n1}, \dots, T_{trn}^{nq}]$$

be the total training period. It is presumed that the power system is under normal operation during time period  $T_{trn}$ . For  $i = 1, 2, \dots, n$ , the collected PMU data flow

$$\{\mathbf{Z}_{i1}, \mathbf{Z}_{i2}, \dots, \mathbf{Z}_{iq}\}$$

are employed for continuous learning of the power system parameters, namely, mean and variance of the proposed test statistic, detection threshold in (12), and then power system state. Specially,

1) *Estimating the relative magnitude and duration of the system event:* Using the proposed test statistic in (10), a system event can be identified with serval samples of PMU data, whenever, the system event indicator satisfies

$$|V_1 - \mu| \geq \gamma, \quad (14)$$

where  $\mu, \gamma = 3\sigma$  are the system-dependent parameters which can be learned from explanatory historical PMU data in the training procedure. The relative magnitude of a system event equals the test statistic  $V_1$ . Given that a system event occurred in sample period  $T_{test}$ , for  $j = 1, 2, \dots, m$ , denote the test data flow as  $\{\mathbf{Z}_{j1}, \mathbf{Z}_{j2}, \dots, \mathbf{Z}_{jq}\}$ , the duration of the event can be roughly estimated by

$$T_{dur} = \sum_{j=1}^m q * T * \omega_j, \quad (15)$$

where

$$\omega_j = \begin{cases} 1, & |V_1 - \mu| \geq \gamma \\ 0, & |V_1 - \mu| < \gamma \end{cases}.$$

2) *Determination of the most sensitive PMU:* According to the data analysis in III-C1, the voltage event addressed on a power system can be identified. Then, in this section, determination of the most sensitive PMU with respect to a system event is another important part to be investigated.

The fact that every fault has its own effect on a power system [25] stimulates us to find the location of most sensitive PMU. According to the data analysis in Section III-C1, we are able to determine the time when the system event occurred, say,  $T_1$ . Assume that the power system operates under normal condition during the time period of  $T_1 - 1$  and there are  $p$  types of influential factors during a sampling time  $T_1$ . Denote  $\mathbf{Z}^{(i)} = \{\mathbf{Z}_{i1}, \mathbf{Z}_{i2}, \dots, \mathbf{Z}_{iq}\}$ ,  $\mathbf{Z}^{(j)} = \{\mathbf{Z}_{j1}, \mathbf{Z}_{j2}, \dots, \mathbf{Z}_{jq}\}$  and  $\mathbf{Z}^{(k)} = \{\mathbf{Z}_{k1}, \mathbf{Z}_{k2}, \dots, \mathbf{Z}_{kq}\}$  as the PMU data flow collected during sample time  $T_1 - 2, T_1 - 1$  and  $T_1$ . For  $l = 1, 2, \dots, p$ , the measured data of each factor are formed as a row vector  $\mathbf{c}_l^{(T)}$ . In order to reveal the most sensitive PMU, we form a factor matrix by duplicating  $\kappa$  times for each factor  $\mathbf{c}_l^{(T_1)}$ , say,

$$\mathbf{C}^{(T_1)} = \begin{bmatrix} \mathbf{c}_1^{(T_1)} \\ \vdots \\ \mathbf{c}_p^{(T_1)} \end{bmatrix}_{\kappa \times N}, \quad (16)$$

where the parameter  $N = q * n_g$ ,  $\kappa = r \log p$  and  $r$  is the rank of  $\mathbf{Z}^{(j)}$ . For  $l = 1, 2, \dots, p$ , we can construct two expansion matrices for parallel data analysis, formulated by

$$\mathbf{A}_1^{(l)} = \begin{bmatrix} \mathbf{Z}^{(i)} \\ \mathbf{C}^{(T_1)} \end{bmatrix}, \mathbf{A}_2^{(l)} = \begin{bmatrix} \mathbf{Z}^{(j)} \\ \mathbf{C}^{(T_1)} \end{bmatrix}. \quad (17)$$

Substitute data flows  $\mathbf{A}_{1l}$  and  $\mathbf{A}_{2l}$  into the test statistic in (10), the location of most sensitive PMU data (denoted as  $loc$ ) during the sample time  $T_1$  can be expressed as

$$loc = \text{index} \left( \max_{l=1,2,\dots,p} \left( V_1^{(l)} \right) \right), \quad (18)$$

where  $\text{index}(x_j) = j$ .

For the readers' convenience, the technological process of the proposed test statistic for voltage stability assessment is summarized in the following:

---

**Implementation of the proposed voltage stability evaluation**

---

- 1): In the training period, collected the PMU data and represent them using (4);
  - 2): System-dependent parameters learning:
    - 2a): for  $i = 1, 2, \dots, n$ , acquire the data flow  $\mathbf{Z}_{i1}, \mathbf{Z}_{i2}, \dots, \mathbf{Z}_{iq}$ ;
    - 2b): calculate the test statistic of the data flow using (10);
    - 2c): calculate mean and variance of the proposed test statistic;
    - 2d): determine the event indicator threshold  $\gamma$  using (14);
  - 3): System event indicating:
    - 3a): acquire the test data flow:  $\mathbf{Z}_{j1}, \dots, \mathbf{Z}_{jq}, j = 1, 2, \dots, m$ ;
    - 3b): calculate the test statistic of the data flow using (10);
    - 3c): determine whether there is an event using (14);
      - if no event detected:
        - add the test data flow into history data;
        - go back to the step 2);
      - else:
        - go to step 4);
  - 4): Determine the relative magnitude, duration and location of the system event using (10), (15) and (18), respectively;
  - 5): FAR (12) and DR (13) analysis;
  - 6): the effect of measurements noise analysis;
  - 7): the effect of parameter  $q$  analysis;
- 

So far, the voltage stability assessment by the proposed test statistic is established. Case studies to evaluate the practical performance of the proposed test statistic will be depicted in detail in the following section.

#### IV. CASE STUDIES

The proposed test statistic for voltage stability assessment is numerically evaluated by the power network benchmarks, namely the IEEE 30-, 118-bus system, a Polish 2383-bus system [28] and a real 34-PMU system. With respect to the synthetic data, the admittance matrices and the underlying power system states are generated by MATPOWER package [29]. It is noted that measurements noise is simulated as uncorrelated Gaussian or Gama distribution with standard deviation per component 0.05 for voltages [25, 29]. We report results from case studies which are designed to evaluate the performance of the proposed test for voltage stability assessment in the following.

##### A. Effect of measurement noise on the voltage stability assessment

Assuming that the power system operates under normal state, we firstly investigate the effect of measurement noise and window size on the voltage stability using synthetic data. With respect to the proposed test in (10), we generated  $p$ -dimensional data independent multivariate data model using the linearized measurement model in (3). Let  $\mathbf{z}_0$  be the initial state of the power system. The nominal significance level [25]

of the data and parameter  $q$  are set to 5% and 5, respectively. For  $i = 1, 2, \dots, n_g$ , we considered two scenarios regarding the innovation random vector  $\mathbf{z}^{(i)}$ :

- 1)  $\mathbf{z}^{(i)}$  are  $p$ -dimensional normal random vector with mean  $\mathbf{z}_0$  and variance  $\text{diag}\{0.05\mathbf{z}_0\}$ .
- 2)  $\mathbf{z}^{(i)} = [z_1^{(i)}, \dots, z_p^{(i)}]$  consists of independent random variables  $z_j^{(i)}$  which are standard Gamma( $\mathbf{z}_0, 0.2236$ ) +  $0.7764\mathbf{z}_0$  random variables.

It is noted that the proposed test statistic imposes no restriction on the relationship between the data dimension and sample size. To mimic the buses deployed in the power system, we have  $p \in \{30, 118, 2383\}$ . A wide range of sample window size was denoted as  $n_g \in \{30, 100, 300, 1000, 2500\}$ . The simulation results reported in this section were based on 1000 independent Monte Carlo simulations.

The simulation results reported in Tab. I and Tab. II showed that DR of the covered test statistics were increased as the dimension and sample sizes became larger. Many entries of the DR of the tests approached to 1 both in the scenarios of Gaussian distributed noise (GSN) and Gama distributed noise (GMN). Besides, we observed from Tab. I and Tab. II that the FAR of the proposed test converged to the nominal 5% quite rapidly while the convergence of the FAR to the nominal level was slower than the normally distributed case. On the other hand, the LR test was not applicable for  $p \geq n_g$  and CLRT test showed slower convergence than the proposed test. In other words, the proposed test statistic had quite accurate DR and robust FAR in a quite wider range of dimensionality and distributions while the LR test and the CLR test are vulnerable to variation of data dimension and noise distribution. Theses could be understood as the proposed test is both asymptotic and nonparametric.

TABLE I: DR and FAR of the test statistics with GSN.

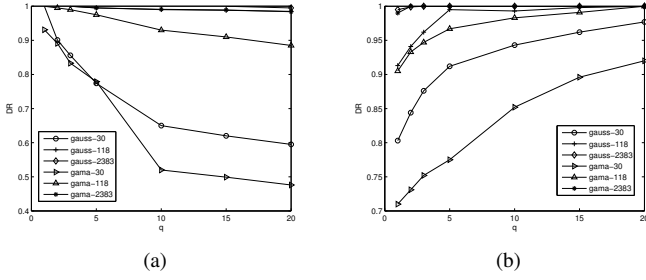
$(p, n, q)$	<i>LR test</i>		<i>CLR test</i>		<i>Proposed test</i>	
	DR	FAR	DR	FAR	DR	FAR
(30,30,10)	0.595	0.059	0.651	0.067	0.694	0.061
(30,100,10)	0.742	0.064	0.899	0.061	0.912	0.058
(30,300,10)	0.901	0.089	0.955	0.057	0.979	0.047
(30,1000,10)	0.958	0.134	0.997	0.054	0.999	0.039
(30,2500,10)	1	0.296	1	0.049	1	0.049
(118,30,10)	-	-	0.924	0.047	0.985	0.059
(118,100,10)	-	-	0.957	0.051	0.993	0.055
(118,300,10)	0.995	0.149	0.993	0.053	1	0.049
(118,1000,10)	1	0.390	1	0.048	1	0.045
(118,2500,10)	1	0.483	1	0.045	1	0.043
(2383,30,10)	-	-	0.991	0.063	0.995	0.058
(2383,100,10)	-	-	1	0.055	1	0.053
(2383,300,10)	-	-	1	0.051	1	0.050
(2383,1000,10)	-	-	1	0.046	1	0.048
(2383,2500,10)	1	0.891	1	0.047	1	0.049

##### B. Effect of the parameter $q$ on the voltage stability assessment

As depicted in the Section II, the parameter  $q$  is an important factor for voltage assessment. Here more details illustrated by experimental data is shown in the following. We fixed the total data size as 600, that is  $q * n_g = 600$  in first experiment while set the window size  $n_g$  as 100 in the second one. Two

TABLE II: DR and FAR of the test statistics with GMN.

$(p, n, q)$	<i>LR test</i>		<i>CLR test</i>		<i>Proposed test</i>	
	DR	FAR	DR	FAR	DR	FAR
(30,30,10)	0.471	0.067	0.553	0.073	0.476	0.069
(30,100,10)	0.660	0.163	0.643	0.075	0.775	0.067
(30,300,10)	0.791	0.289	0.816	0.067	0.891	0.066
(30,1000,10)	0.958	0.334	0.894	0.060	0.953	0.063
(30,2500,10)	0.996	0.596	0.934	0.057	0.989	0.055
(118,30,10)	-	-	0.801	0.066	0.885	0.059
(118,100,10)	-	-	0.879	0.059	0.967	0.063
(118,300,10)	0.932	0.349	0.942	0.063	0.995	0.056
(118,1000,10)	0.999	0.875	0.970	0.056	1	0.052
(118,2500,10)	1	0.977	0.998	0.051	1	0.055
(2383,30,10)	-	-	0.947	0.062	0.984	0.061
(2383,100,10)	-	-	0.983	0.058	0.999	0.060
(2383,300,10)	-	-	1	0.059	1	0.054
(2383,1000,10)	-	-	1	0.049	1	0.052
(2383,2500,10)	1	1	1	0.046	1	0.048

Fig. 2: Effect of the parameter  $q$  on the voltage stability assessment.

kind of measurements noise as shown in the Section IV-A were considered. It is noted that the notations *gauss* – 30 and *gama* – 30 in Fig. 2a and Fig. 2b mean that the measurements noise adopted are GSN and GMN with the number of PMUs is  $p = 30$ , respectively. Similar definitions also work for other notations, i.e., *gauss* – 118, *gama* – 118, *gauss* – 2383 and *gama* – 2383.

Fig. 2a shows that the DR decreased as  $q$  increasing for the first experiment while Fig. 2b illustrates that DR showed positive response to the increase of  $q$  in the second one. The selection of medium size  $q$  is the trade-off between the DR and realtime performance. In the rest experiment, we set the parameter  $q$  as  $q = 5$ .

### C. Online Voltage Stability Assessment Using the Synthetic Data

The performance of voltage stability assessment using the proposed test statistic was evaluated by the simulated data generated from IEEE 30-bus, IEEE 118-bus and a polish 2383-bus system, respectively. The specific details of the systems are referred to the case30.m, case118.m and case2383.m in Matpower package and Matpower 5.1-User's Manual [30]. In the simulations, changes on the active load of each bus were considered as potential factors. Besides, each change of a factor was described as a signal. Three kinds of signals that affected the operating state of the test system were considered. For simplicity, the signals for each factor are shown in Tab.

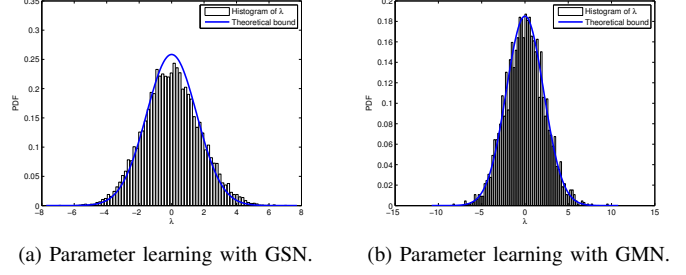


Fig. 3: Parameter learning of IEEE 118-bus system

III, IV and V.  $\rho$  denotes the number of P-V node in the test systems and is chosen on a random basis. For the sake of simplicity, the case study based on the IEEE 118-bus system is presented below. The results generated from IEEE 30-bus system and the Polish 2383-bus system were deferred to the Appendix C.

TABLE III: Signal Type I: Voltage Dip

Bus	Duration	Active Load (MW)
$\rho$	$t = 1 \sim 300$	40.0
	$t = 301 \sim 600$	80
	$t = 601 \sim 1000$	120
Others	$t = 1 \sim 1000$	Unchanged

TABLE IV: Signal Type II: Voltage Swell

Bus	Duration	Active Load (MW)
$\rho$	$t = 1 \sim 300$	-10.0
	$t = 301 \sim 540$	-25.1
	$t = 541 \sim 780$	-39.3
	$t = 781 \sim 900$	-62.7
	$t = 901 \sim 1000$	-75.3
Others	$t = 1 \sim 1000$	Unchanged

TABLE V: Signal Type III: Voltage Dip and Swell

Bus	Duration	Active Load (MW)
$\rho$	$t = 1 \sim 300$	10.0
	$t = 301 \sim 600$	60.0
	$t = 601 \sim 900$	120.0
	$t = 901 \sim 1000$	35.0
Others	$t = 1 \sim 1000$	Unchanged

The signals were generated in load of P-V node  $\rho = 63$  for the case of IEEE 118-bus system. During the training period, a total of 5min data were collected when the system is under normal condition. Let  $p = 118, n_g = 100, q = 5$ . Two kind of measurements noise as shown in the Section IV-A were considered. As shown in the Section III-B, the proposed test statistic satisfies  $\lambda \xrightarrow{d} \mathcal{N}(0, 1)$ . The theoretical bound in Fig.3 is the probability density function (PDF) of  $\lambda$ . Fig.3 shows that the mean and variance of  $\lambda$  fits fabulously with theoretical ones.

The voltage stability assessment began at 301 s. 60 seconds of data were collected. Three kind of system events were

generated in load of 63<sup>th</sup> bus from 320s to 340s, respectively. According to the results in Fig.9 and event indicators (14) and (15), we can know that the event occurred at 301s and the actual duration of the signals can be calculated as  $t_{dur} = 1000/(q * n_g) * 10 = 20s$ . Based on above analysis, we can then determine the location of the most sensitive bus using (18). The results in Fig.4 demonstrated that 63<sup>th</sup> bus was the most sensitive bus in presence of all three kinds system events when the measurements noise was set as GSN or GMN.

#### D. A Real Data Analysis

In this section, we evaluate the efficacy of the proposed test statistic for power system stability. For the experiments shown in the following, the real power flow data is of a chain-reaction fault happened in the China power grids in 2013. The PMU number, the sample rate and the total sample time are  $p = 34$ ,  $K = 50Hz$  and 284s, respectively. The chain-reaction fault happened from  $t = 65.4s$  to  $t = 73.3s$ .

Fig. 5 and Fig. 6 illustrate the three-dimensional power flow data in the stable state and the fault state, respectively. It is seen that the power flow varies smoothly in the stable state while the power flow changes irregularly in the fault state. Let  $q = 5, n_g = 50$ . Fig.7 shows that the mean and variance of  $\lambda$  agrees well with theoretical ones. Based on the results in Fig.7 and event indicators (14) and (15), the occurrence time and the actual duration of the event can be identified as  $t_0 = 65s$  and  $t_{dur} \approx 8s$ , respectively. Similar to the data analysis above, we can then determine the location of the most sensitive bus using (18). The result shown in Fig.8 illustrate that 17<sup>th</sup> and 18<sup>th</sup> PMU are the most sensitive PMUs which is in accordance with the actual accident situation.

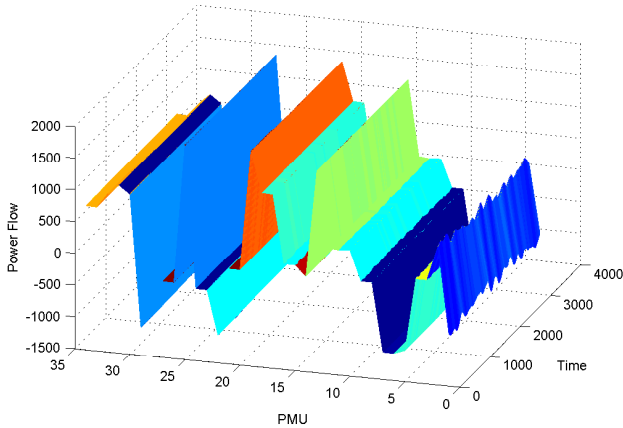


Fig. 5: The realistic 34-PMU power flow under normal condition.

#### V. CONCLUSION

Motivated by the immediate demands of the big data analysis for large scale smart grids, this paper proposed a real time data-driven method to indicate the voltage stability from massive streaming PMU data. Firstly, we represent the PMU data as a sequence of large random matrices. This is a crucial

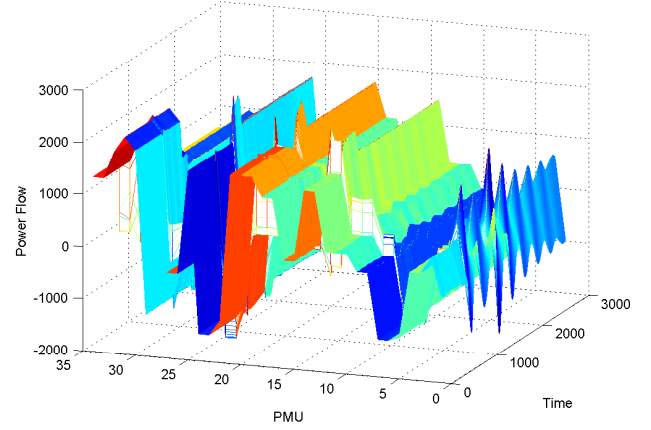


Fig. 6: The realistic 34-PMU power flow around events occurrence.

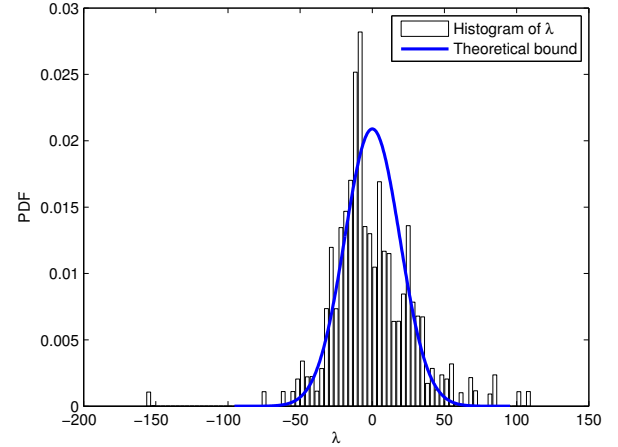


Fig. 7: Parameter learning of the real 34-PMU system.

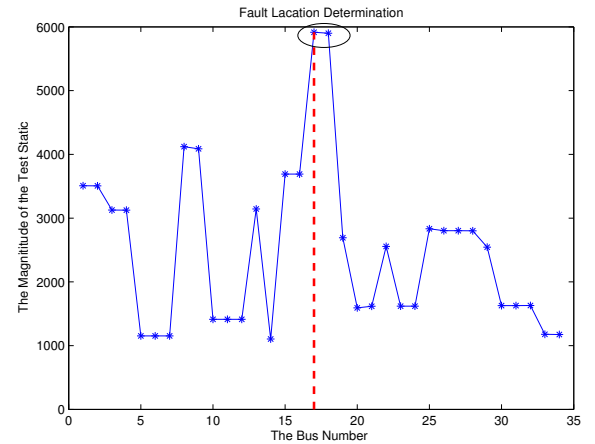


Fig. 8: Determination of most sensitive bus for the real 34-PMU system.



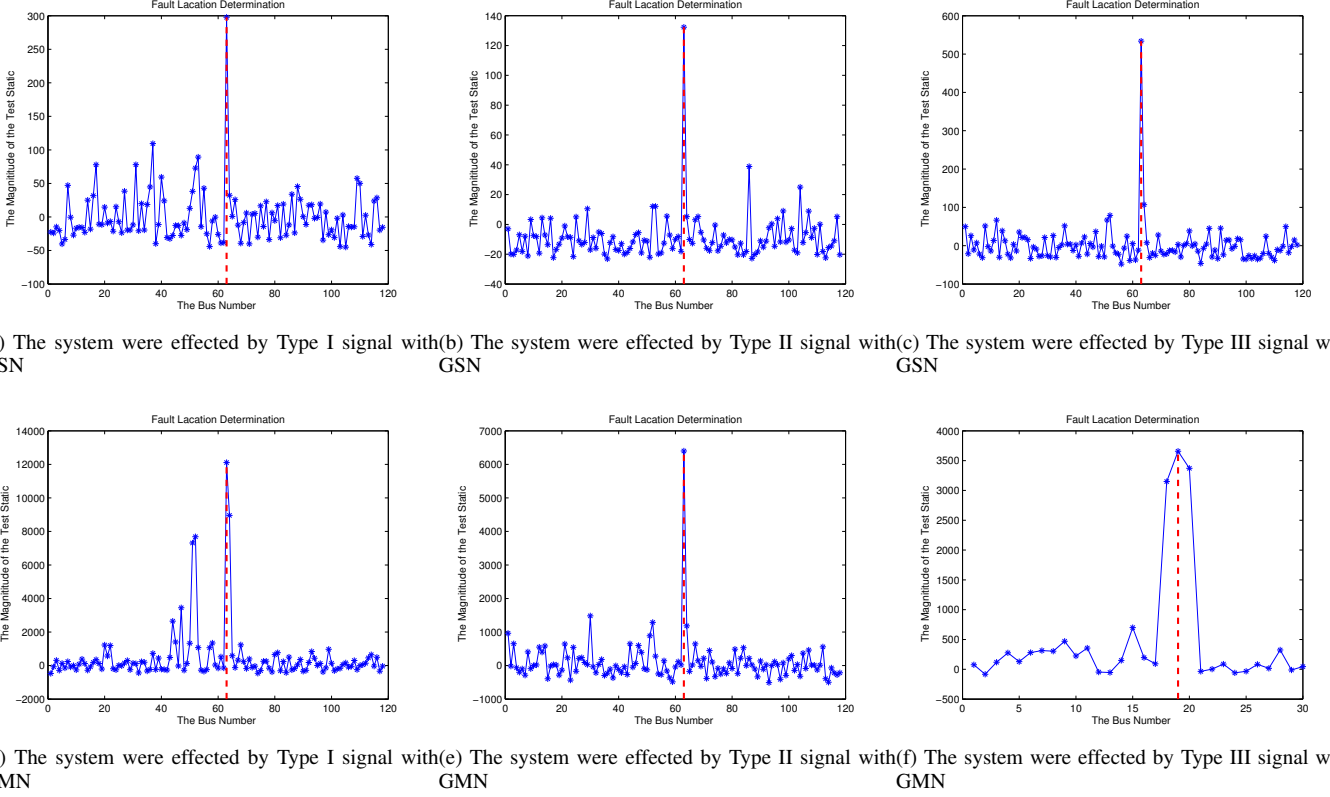


Fig. 4: Determination of most sensitive bus for IEEE 118-bus system

part for voltage stability assessment as it turning the big PMU data into tiny data for the practical use. Rather than employing the raw PMU data or window-truncated data, a comprehensive analysis of PMU data flow, namely, multiple high-dimensional test, is then proposed to indicate the voltage stability state. The proposed test statistic is of widespread practical value and great practical significance as: it can jointly reveal the relative magnitude, duration and location of a system event in polynomial time due to principal component calculation and redundant computation elimination; it is nonparametric without assuming a specific parameter distribution for the PMU measurements; it imposes no restriction on the relationship between the data dimension and sample size. Besides, the case studies based on synthetic data and real data illustrate and demonstrate the superiority of proposed voltage stability indicator.

The current work provides a fundamental exploration of data analysis for massive streaming PMU data. Much more attentions are to be paid along this research direction, such as classification of power events from massive streaming PMU data. It is also noted that this work is a data-driven method which is a new substitute for power system state estimation. The combination of power system scenario analysis and the data driven methods is encouraged to be investigated for better understanding of the power system state.

## APPENDIX A

### THE TRADITIONAL HIGH-DIMENSIONAL COVARIANCE TESTS

For the readers' convenience, we give a brief description of the likelihood ratio (LR) test statistic and correction of the likelihood ratio (CLR) test statistic in the following.

Let  $\sum_{g=1}^q n_g = n$  be the total sample size,  $\bar{\mathbf{z}}_g = \frac{1}{n_g} \sum_{k=1}^{n_g} \mathbf{z}_{gk}$ ,

$$\mathbf{Y}_g = \frac{1}{n_g - 1} \sum_{k=1}^{n_g} (\mathbf{z}_{gk} - \bar{\mathbf{z}}_g) (\mathbf{z}_{gk} - \bar{\mathbf{z}}_g)' \quad (19)$$

$$\mathbf{Y} = \sum_{g=1}^q \mathbf{Y}_g.$$

The LR test [17] for testing (5) is

$$V_2 = \frac{\prod_{g=1}^q |\mathbf{Y}_g|^{\frac{1}{2} N_g}}{|\mathbf{Y}|^{\frac{1}{2} M}}, \quad (20)$$

where

$$N_g = n_g - 1, \quad M = N_1 + N_2 + \cdots + N_q = n - q.$$

It is noted that the calculation of the numerator and denominator of  $V_2$  will lead to overflow as  $n_g$  becomes large. To overcome the overflow difficulty, a CLR test [19] for testing



the equality of more population covariance matrices is shown as follows. Let

$$V_{2h} = \frac{|\mathbf{Y}_1 + \mathbf{Y}_2 + \cdots + \mathbf{Y}_{h-1}|^{\frac{1}{2}(N_1+N_2+\cdots+N_{h-1})} |\mathbf{Y}_h|^{\frac{1}{2}N_h}}{|\mathbf{Y}|^{\frac{1}{2}M}}, \quad (21)$$

where  $h = 2, 3, \dots, q$ . Then  $V_2 = \prod_{h=2}^q V_{2h}$ .

The CLR test statistic is

$$V_3 = \sum_{h=2}^q -\frac{2}{N_1 + N_2 + \cdots + N_{h-1}} \log T_{1h} - pf(y_{1h}, y_{2h}), \quad (22)$$

where

$$y_{1h} = \frac{p}{N_1 + N_2 + \cdots + N_{h-1}}, y_{2h} = \frac{p}{N_h}$$

and

$$\begin{aligned} f(y_1, y_2) &= \frac{y_1 + y_2 - y_1 y_2}{y_1 y_2} \log \left( \frac{y_1 + y_2}{y_1 + y_2 - y_1 y_2} \right) \\ &+ \frac{y_1^2 (1 - y_2) \log(1 - y_2) + y_2^2 (1 - y_1) \log(1 - y_1)}{y_1 y_2 (y_1 + y_2)} \\ &- \frac{y_1}{y_1 + y_2} \log \frac{y_1}{y_1 + y_2} - \frac{y_2}{y_1 + y_2} \log \frac{y_2}{y_1 + y_2}. \end{aligned}$$

## APPENDIX B

### COMPUTATION ASPECT OF THE PROPOSED TEST STATISTIC

From (7) and (8), we can know that the computational complexity of calculating the test statistics  $A_s$ ,  $A_t$  and  $C_{st}$  are  $O(\varepsilon_1 n_g^4)$ ,  $O(\varepsilon_2 n_g^4)$  and  $O(\varepsilon_3 n_g^4)$ , respectively. With the increasing scale of PMU deployment and the increasing complexity of issues addressed by it, which is a new raised and huge challenge for voltage stability assessment and quality control of power system. Here, we propose a lower complexity method to calculate  $A_s$ ,  $A_t$  and  $C_{st}$  by by redundant computation elimination and principal component calculation. Technical details are elaborated in the following.

#### A. Redundant Computation Elimination

We firstly consider eliminating the index-wise redundant computation during calculating the term  $A_{l,\{l=s,t\}}$ .

Let

$$\begin{aligned} A_{l1} &= \frac{1}{n_g (n_g - 1)} \sum_{i \neq j} (\mathbf{z}'_{li} \mathbf{z}_{lj})^2, \\ A_{l2} &= \frac{2}{n_g (n_g - 1) (n_g - 2)} \sum_{i,j,k}^* \mathbf{z}'_{li} \mathbf{z}_{lj} \mathbf{z}'_{lj} \mathbf{z}_{lk}, \end{aligned}$$

and

$$A_{l3} = \frac{1}{n_g (n_g - 1) (n_g - 2) (n_g - 3)} \sum_{i,j,k,h}^* \mathbf{z}'_{li} \mathbf{z}_{lj} \mathbf{z}'_{lk} \mathbf{z}_{lh}.$$

It is easy to find that indices  $i, j, k, l$  in  $A_{l1}$ ,  $A_{l2}$  and  $A_{l3}$  are invariant with respect to the swapping places. Let

$$\begin{aligned} \Omega_1 &= \{\{i, j\} : 1 \leq i, j \leq n_g, i \neq j\}, \\ \Omega_2 &= \{\{i, j, k\} : 1 \leq i, j, k \leq n_g, i \neq j \neq k\}, \\ \Omega_3 &= \{\{i, j, k, h\} : 1 \leq i, j, k, h \leq n_g, i \neq j \neq k \neq h\}. \end{aligned}$$

Specially, we are to determine unrepeated sets of the indices from  $\Omega_1$ ,  $\Omega_2$  and  $\Omega_3$  when calculating  $A_{l1}$ ,  $A_{l2}$  and  $A_{l3}$ . Following the permutations and combinations principle in [31], the unrepeated ensembles can be expressed as

$$\begin{aligned} \dot{\Omega}_1 &= \{\{i, j\} : 2 \leq i \leq n_g, 1 \leq j \leq i - 1\}, \\ \dot{\Omega}_2 &= \{\{i, j, k\} : 3 \leq i \leq n_g, 2 \leq j \leq i - 1, 1 \leq k \leq j - 1\}, \\ \dot{\Omega}_3 &= \left\{ \{i, j, k, h\} : \{4 \leq i \leq n_g, 3 \leq j \leq i - 1\} \cup \{2 \leq k \leq j - 1, 1 \leq h \leq k - 1\} \right\}. \end{aligned}$$

Let  $Q_{n_g}^r = n_g! / (n_g - r)!$ . Then,  $A_{l1}$ ,  $A_{l2}$  and  $A_{l3}$  can be expressed by

$$A_{l1} = \frac{2}{Q_{n_g}^2} \sum_{\{i,j\} \in \dot{\Omega}_1} (\mathbf{z}'_{li} \mathbf{z}_{lj})^2,$$

$$A_{l2} = \frac{6}{Q_{n_g}^3} \sum_{\{i,j,k\} \in \dot{\Omega}_2} \mathbf{z}'_{li} \mathbf{z}_{lj} \mathbf{z}'_{lj} \mathbf{z}_{lk},$$

and

$$A_{l3} = \frac{24}{Q_{n_g}^4} \sum_{\{i,j,k,h\} \in \dot{\Omega}_3} \mathbf{z}'_{li} \mathbf{z}_{lj} \mathbf{z}'_{lk} \mathbf{z}_{lh}.$$

As a result, the computation complexity of calculating  $A_{l1}$ ,  $A_{l2}$  and  $A_{l3}$  is reduced by a factor of  $1/2$ ,  $1/6$  and  $1/24$  compared with direct manipulation, respectively.

Besides, we notice that manipulation of  $A_{l1}$ ,  $A_{l2}$  and  $A_{l3}$  is completed in sequence and this manipulation is inefficient because of the repeated vector multiplication operations. For instance, vector multiplication  $\mathbf{z}'_{li} \mathbf{z}_{lj}$  is repeated many times when calculating  $A_{l1}$ ,  $A_{l2}$  and  $A_{l3}$ . This kind of repeated calculation can be avoided by the following steps.

Let  $\mathbf{Z}^l$  be voltage-relevant matrix whose elements are

$$Z_{ij}^l = \mathbf{z}'_{li} \mathbf{z}_{lj}, \{i, j\} \in \dot{\Omega}_1.$$

Then  $A_{l1}$ ,  $A_{l2}$  and  $A_{l3}$  can be equivalently denoted as

$$A_{l1} = \frac{2}{Q_{n_g}^2} \sum_{\{i,j\} \in \dot{\Omega}_1} (Z_{ij}^l)^2,$$

$$A_{l2} = \frac{6}{Q_{n_g}^3} \sum_{\{i,j,k\} \in \dot{\Omega}_2} Z_{ij}^l Z_{jk}^l,$$

and

$$A_{l3} = \frac{24}{Q_{n_g}^4} \sum_{\{i,j,k,h\} \in \dot{\Omega}_3} Z_{ij}^l Z_{kh}^l.$$

The aforementioned equivalent expression means that we can compute  $\mathbf{z}'_{li} \mathbf{z}_{lj}$  only once during the progress in calculating  $A_{l1}$ ,  $A_{l2}$  and  $A_{l3}$ . Thus the computing time were reduced to  $1/n_g^2$  of the conventional calculation of  $A_{l2}$  and  $A_{l3}$ .

Similarly, the computation burden of calculating  $C_{s,t}$  can be also alleviated by repeating the above steps. Here we only provide the result.  $C_{s,t}$  can be equivalently denoted as

$$\begin{aligned} C_{s,t} &= \frac{2}{n_g^2} \sum_{\{i,j\} \in \dot{\Omega}_1} (Y_{ij})^2 \\ &- \frac{12}{n_g Q_{n_g}^2} \sum_{\{i,j,k\} \in \dot{\Omega}_2} (Y_{ij} Y'_{jk} + Y'_{ij} Y_{jk}) \\ &+ \frac{24}{(Q_{n_g}^2)^2} \sum_{\{i,j,k,h\} \in \dot{\Omega}_3} Y_{ij} Y_{kh}, \end{aligned}$$

where  $Y_{ij} = \mathbf{z}_{si}' \mathbf{z}_{tj}$ ,  $\{i, j\} \in \dot{\Omega}_1$ .

### B. Principal Component Calculation

Let  $A = B + C$ , where  $A, B, C$  are positive random variables. Let  $n_g$  be a large positive number, say, 100. If condition that  $C/B < 1/n_g$  is satisfied, then  $B$  is called the principal component of  $A$ . Then we introduce the principal component calculation.

It is noted that the magnitude of voltage measurements are positive, that is,

$$Z_{kj}^l > 0, \{i, j\} \in \{\dot{\Omega}_1 \cup \dot{\Omega}_2 \cup \dot{\Omega}_3\},$$

then

$$\sum_{\{i,j\} \in \dot{\Omega}_1} (Z_{ij}^l)^2 > \sum_{\{i,j,k\} \in \dot{\Omega}_2} Z_{ij}^l Z_{jk}^l > \sum_{\{i,j,k,h\} \in \dot{\Omega}_3} Z_{ij}^l Z_{kh}^l.$$

For  $n_g \gg 1$ , divide  $A_{l2}$  and  $A_{l3}$  by  $A_{l1}$ , respectively, we can get

$$\begin{aligned} \frac{A_{l2}}{A_{l1}} &= \frac{\frac{6}{Q_{n_g}^3} \sum_{\{i,j,k\} \in \dot{\Omega}_2} Z_{ij}^l Z_{jk}^l}{\frac{2}{Q_{n_g}^2} \sum_{\{i,j\} \in \dot{\Omega}_1} (Z_{ij}^l)^2} < \frac{3}{n_g - 2} \ll 1, \\ \frac{A_{l3}}{A_{l1}} &= \frac{\frac{24}{Q_{n_g}^4} \sum_{\{i,j,k,h\} \in \dot{\Omega}_3} Z_{ij}^l Z_{kh}^l}{\frac{2}{Q_{n_g}^2} \sum_{\{i,j\} \in \dot{\Omega}_1} (Z_{ij}^l)^2} > \frac{12}{(n_g - 2)(n_g - 3)} \ll 1. \end{aligned} \quad (23)$$

From (23), it is known that  $A_{l1}$  is the principal component to be computed when computing  $A_l$ . We can get similar result when calculating  $C_{s,t}$ . Above all, the simplified test statistic can be represented as

$$V_1 = \sum_{\{i,j\} \in \dot{\Omega}_1} \frac{2}{Q_{n_g}^2} \left( (Z_{ij}^1)^2 + (Z_{ij}^p)^2 \right) - \frac{2}{n_g^2} (Y_{ij})^2. \quad (24)$$

Let  $\varepsilon = \varepsilon_1 + \varepsilon_2 + \varepsilon_3$ . It is noted that this kind approximate computation will reduce the computation from  $O(\varepsilon n_g^4)$  to  $O(\eta n_g^2)$ . The price paid for such an operation is that the simplified statistic in (24) is no longer unbiased.

## APPENDIX C

### ADDITIONAL CASE STUDY RESULTS

The signals were generated in load of P-V node  $\rho = 19$  and  $\rho = 1044$  for the case of IEEE 30-bus and the Polish 2383-bus system, respectively. Other experimental conditions were the same as the tests for the IEEE 118-bus system. The experiment results are shown in Fig.9, Fig.10, Fig.11 and Fig.12.

## REFERENCES

- [1] V. Terzija, G. Valverde, D. Cai, P. Regulski, V. Madani, J. Fitch, S. Skok, M. M. Begovic, and A. Phadke, "Wide-area monitoring, protection, and control of future electric power networks," *Proceedings of the IEEE*, vol. 99, no. 1, pp. 80–93, 2011.
- [2] R. C. Qiu and P. Antonik, *Smart Grid and Big Data: Theory and Practice*. Hoboken, NJ, USA: John Wiley & Sons, 2015.

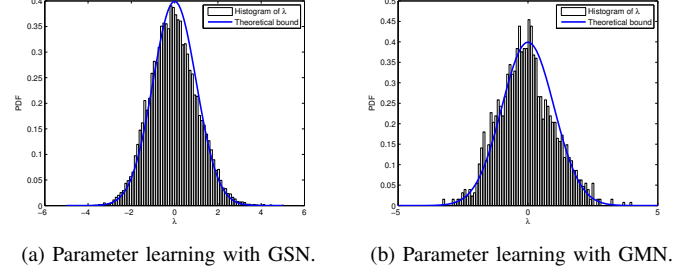


Fig. 9: Parameter learning of IEEE 30-bus system

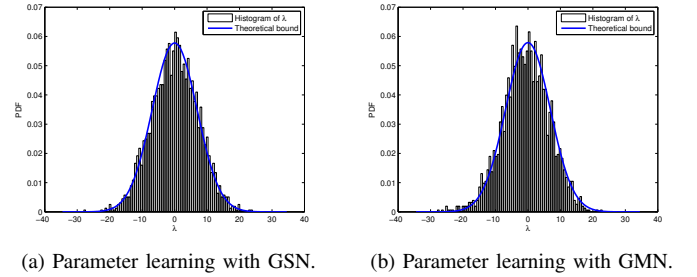
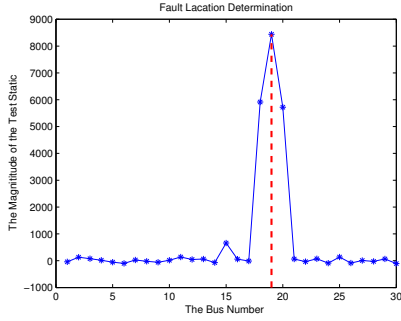
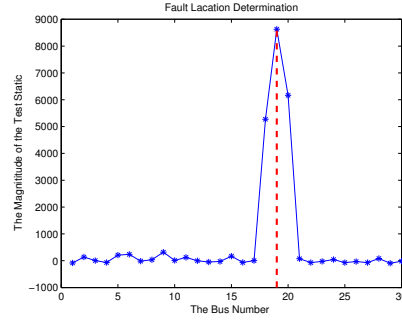


Fig. 11: Parameter learning of the Polish 2383-bus system

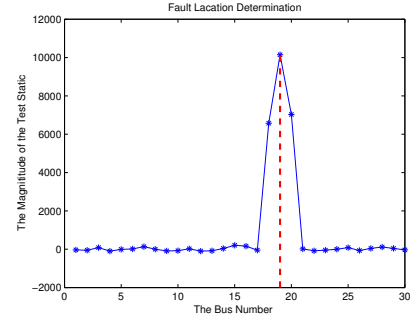
- [3] C. Lu, B. Shi, X. Wu, and H. Sun, "Advancing china's smart grid: Phasor measurement units in a wide-area management system," *IEEE Power and Energy Magazine*, vol. 13, no. 5, pp. 60–71, 2015.
- [4] S. Nuthalapati and A. G. Phadke, "Managing the grid: Using synchrophasor technology [guest editorial]," *IEEE Power and Energy Magazine*, vol. 13, no. 5, pp. 10–12, 2015.
- [5] S. Chakrabarti, E. Kyriakides, T. Bi, D. Cai, and V. Terzija, "Measurements get together," *IEEE Power and Energy Magazine*, vol. 7, no. 1, pp. 41–49, 2009.
- [6] J. De La Ree, V. Centeno, J. S. Thorp, and A. G. Phadke, "Synchronized phasor measurement applications in power systems," *IEEE Transactions on Smart Grid*, vol. 1, no. 1, pp. 20–27, 2010.
- [7] P.-A. Lof, G. Anderson, and D. Hill, "Voltage stability indices for stressed power systems," *IEEE Transactions on Power Systems*, vol. 8, no. 1, pp. 326–335, 1993.
- [8] S. G. Ghiocel and J. H. Chow, "A power flow method using a new bus type for computing steady-state voltage stability margins," *IEEE Transactions on Power Systems*, vol. 29, no. 2, pp. 958–965, 2014.
- [9] I. R. Pordanjani, Y. Wang, and W. Xu, "Identification of critical components for voltage stability assessment using channel components transform," *IEEE Transactions on Smart Grid*, vol. 4, no. 2, pp. 1122–1132, 2013.
- [10] D. H. A. Lee, "Voltage stability assessment using equivalent nodal analysis," *IEEE Transactions on Power Systems*, vol. 31, no. 1, pp. 454–463, 2016.
- [11] X. Xu, X. He, Q. Ai, and R. C. Qiu, "A correlation analysis method for power systems based on random matrix theory," 2015, DOI: 10.1109/TSG.2015.2508506.



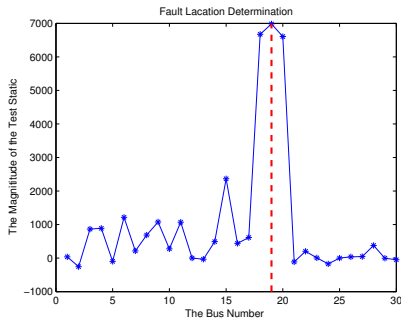
(a) The system were effected by Type I signal with GSN



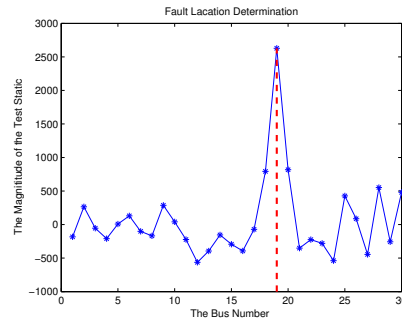
(b) The system were effected by Type II signal with GSN



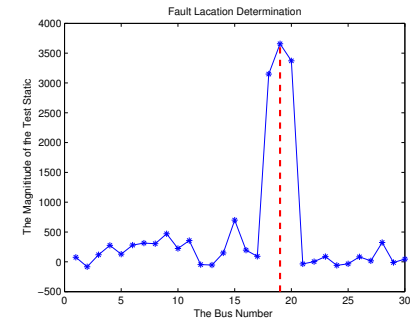
(c) The system were effected by Type III signal with GSN



(d) The system were effected by Type I signal with GMN

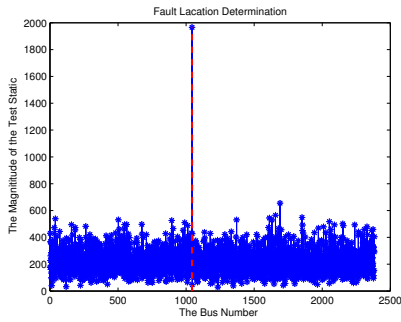


(e) The system were effected by Type II signal with GMN

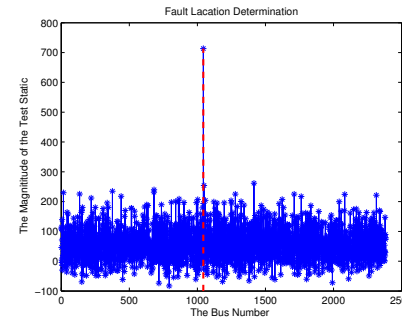


(f) The system were effected by Type III signal with GMN

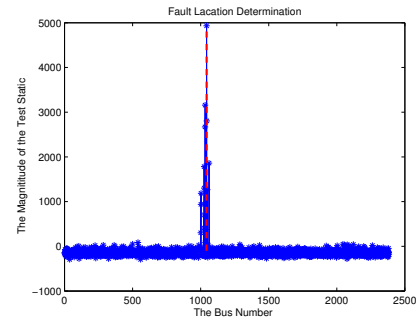
Fig. 10: Determination of most sensitive bus for IEEE 30-bus system



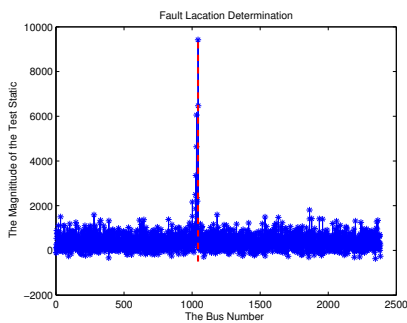
(a) The system were effected by Type I signal with GSN



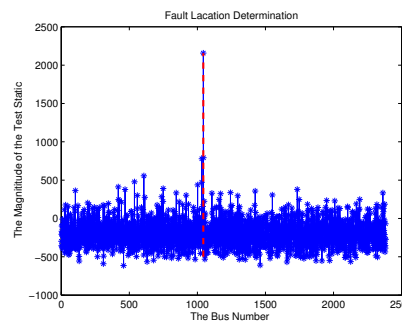
(b) The system were effected by Type II signal with GSN



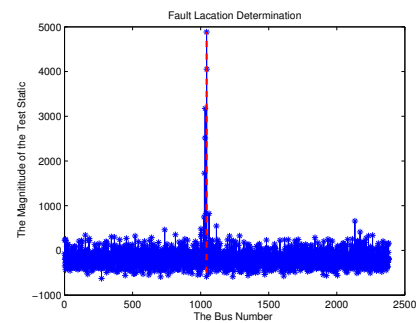
(c) The system were effected by Type III signal with GSN



(d) The system were effected by Type I signal with GMN



(e) The system were effected by Type II signal with GMN



(f) The system were effected by Type III signal with GMN

Fig. 12: Determination of most sensitive bus for the Polish 2383-bus system

- [12] L. Xie, Y. Chen, and P. Kumar, "Dimensionality reduction of synchrophasor data for early event detection: Linearized analysis," *IEEE Transactions on Power Systems*, vol. 29, no. 6, pp. 2784–2794, 2014.
- [13] J. M. Lim and C. L. DeMarco, "Svd-based voltage stability assessment from phasor measurement unit data," *IEEE Transactions on Power Systems*, vol. 31, no. 4, pp. 2557–2565, 2016.
- [14] G. Ghanavati, P. D. Hines, and T. I. Lakoba, "Identifying useful statistical indicators of proximity to instability in stochastic power systems," *IEEE Transactions on Power Systems*, vol. 31, no. 2, pp. 1360–1368, 2016.
- [15] X. He, Q. Ai, R. C. Qiu, W. Huang, L. Piao, and H. Liu, "A big data architecture design for smart grids based on random matrix theory," 2015, DOI: 10.1109/TSG.2015.2445828.
- [16] X. He, R. C. Qiu, Q. Ai, L. Chu, X. Xu, and Z. Ling, "Designing for situation awareness of future power grids: An indicator system based on linear eigenvalue statistics of large random matrices," DOI: 10.1109/AC-CESS.2016.2581838.
- [17] Z. Bai and H. Saranadasa, "Effect of high dimension: by an example of a two sample problem," *Statistica Sinica*, pp. 311–329, 1996.
- [18] A. K. Gupta and J. Xu, "On some tests of the covariance matrix under general conditions," *Annals of the Institute of Statistical Mathematics*, vol. 58, no. 1, pp. 101–114, 2006.
- [19] Z. Bai, D. Jiang, J.-F. Yao, and S. Zheng, "Corrections to lrt on large-dimensional covariance matrix by rmt," *The Annals of Statistics*, pp. 3822–3840, 2009.
- [20] O. Ledoit and M. Wolf, "Some hypothesis tests for the covariance matrix when the dimension is large compared to the sample size," *Annals of Statistics*, pp. 1081–1102, 2002.
- [21] S. X. Chen and Y.-L. Qin, "A two-sample test for high-dimensional data with applications to gene-set testing," *The Annals of Statistics*, vol. 38, no. 2, pp. 808–835, 2010.
- [22] S. X. Chen, L.-X. Zhang, and P.-S. Zhong, "Tests for high-dimensional covariance matrices," *Journal of the American Statistical Association*, 2012.
- [23] A. Lee, "U-statistics," *Theory and Practice*, Marcel Dekker, New York, 1990.
- [24] F. Milano and R. Zárate-Miñano, "A systematic method to model power systems as stochastic differential algebraic equations," *IEEE Transactions on Power Systems*, vol. 28, no. 4, pp. 4537–4544, 2013.
- [25] M. H. Bollen, *Understanding power quality problems*. IEEE press New York, 2000, vol. 3.
- [26] F. Dörfler and F. Bullo, "Kron reduction of graphs with applications to electrical networks," *IEEE Transactions on Circuits and Systems I: Regular Papers*, vol. 60, no. 1, pp. 150–163, 2013.
- [27] P. Kundur, J. Paserba, V. Ajjarapu, G. Andersson, A. Bose, C. Canizares, N. Hatziairgiyriou, D. Hill, A. Stankovic, and C. Taylor, "Definition and classification of power system stability ieee/cigre joint task force on stability terms and definitions," *IEEE transactions on Power Systems*, vol. 19, no. 3, pp. 1387–1401, 2004.
- [28] R. Kavasseri and S. K. Srinivasan, "Joint placement of phasor and power flow measurements for observability of power systems," *IEEE Transactions on Power Systems*, vol. 26, no. 4, pp. 1929–1936, 2011.
- [29] R. D. Zimmerman, C. E. Murillo-Sánchez, and R. J. Thomas, "Matpower: Steady-state operations, planning, and analysis tools for power systems research and education," *IEEE Transactions on power systems*, vol. 26, no. 1, pp. 12–19, 2011.
- [30] R. D. Zimmerman and C. E. Murillo-Sanchez, "Matpower 5.1-user's manual," *Power Systems Engineering Research Center (PSERC)*, 2015.
- [31] M. HALL, "Permutations and combinations," *Combinatorial Theory, Second Edition*, pp. 1–7, 1983.